

Dynamic Response Computation Software



Instruction Manual **5.2 Edition**

National Aeronautics and Space Administration
Lyndon B. Johnson Space Center
Houston, Texas

DIRECT Instruction Manual

Timothy T. Cao, Ph.D.

Structures and Dynamics Branch
Structure Engineering Division

Lyndon B. Johnson Space Center
National Aeronautics and Space Administration

TABLE OF CONTENTS

1. Introduction	1
2. DIRECT Input	3
3. DIRECT Output	18
4. Example	20
4.1 Input Data.....	20
4.2 Output Data	24
5. Mathematical Background	26
5.1 Introduction	26
5.2 Normal Mode Analysis	26
5.2.1 Undamped Systems	26
5.2.2 General Damped Systems	28
5.2.3 Proportionally Damped Systems	29
5.3 DIRECT Ritz Vectors Computation	30
5.4 Techniques in Component Mode Synthesis.....	32
References	34

1. INTRODUCTION

DIRECT is a program originally developed to conduct fast dynamic structural assessment of the Space Shuttle and its payloads under the harsh environment of liftoff and landing events to ensure the safety of the astronauts, the Space Shuttle and the payloads. **DIRECT** has since been utilized in the X38 Crew Return Vehicle design, the International Space Station component assembly and the TRIANA payload analysis. **DIRECT** software has allowed the Space Shuttle, the International Space Station and other program to conduct multiple quick assessment of structural integrity precipitated by late payload manifest changes, weight changes, cargo modifications, and math model upgrades. These changes occur very often during engineering design process.

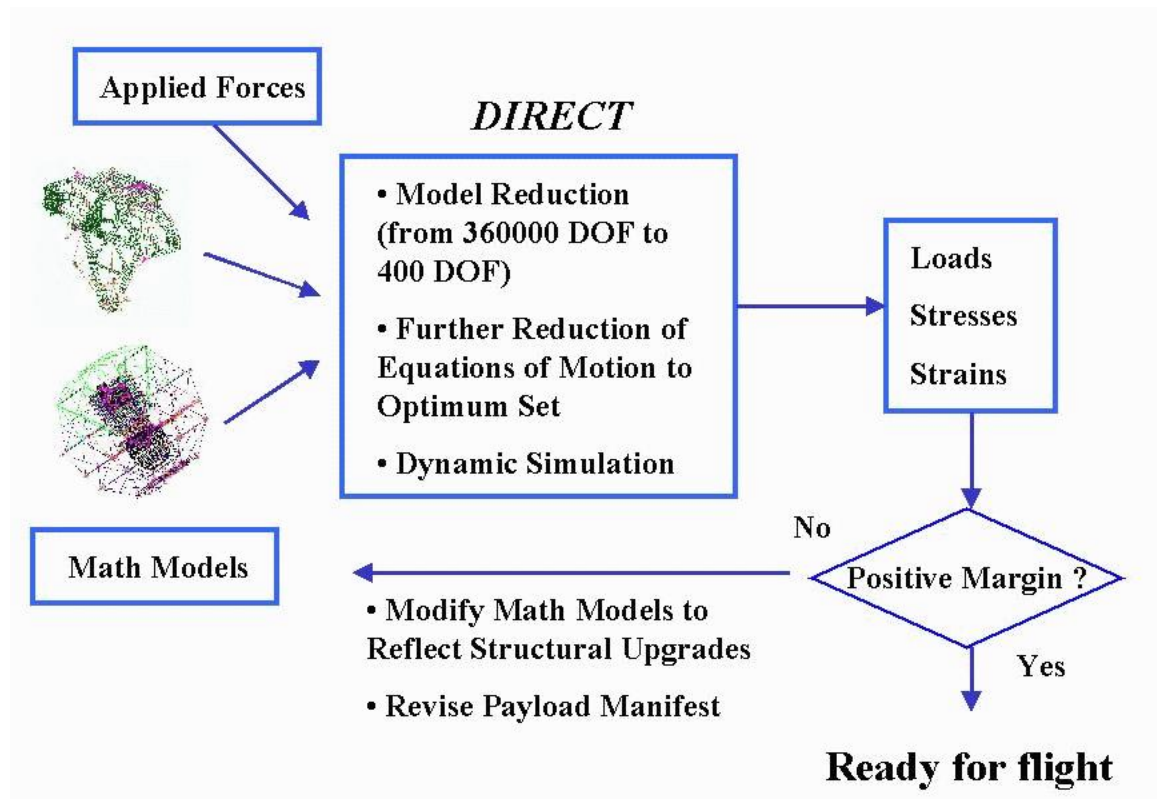


Figure 1.1 **DIRECT** Payload Assessment Process

Ritz vectors represent an alternative to mode shape vectors. In numerical analysis, Ritz vectors have been demonstrated to be superior to normal mode shapes in many structural dynamic analysis applications such as transient response analysis using superposition, model reduction, and component mode synthesis. In **DIRECT** program, a special form of Ritz vectors are utilized for model reduction and component mode synthesis. A flow chart of how **DIRECT** incorporated with the payload assessment process is shown in Figure 1.1.

This instructional manual is divided into five sections. In Section 2, the format and procedure to submit input data are presented. A Graphic User Interface program leads user through a simple set of input data. Output data from **DIRECT** program are explained in Section 3. An example of the Shuttle X38 payloads dynamic simulation is illustrated in Section 4. In Section 5, mathematical background which are utilized through out **DIRECT** program are summarized. First the basic theory of modal analysis is shown. Next, the derivation of Ritz vectors from structural property matrices is presented. Two techniques used in component mode synthesis are briefly presented.

Finally, it is emphasized that although the focus of the interest of **DIRECT** program is the Shuttle-payloads dynamic loads analysis problem, it can be used for any other combined structural system such as commercial expendable and reusable launch vehicles, automobiles, aircrafts, earthquake resistant building, and marine structures.

2. DIRECT INPUT

The first screen a user sees when using the Graphical User Interface (GUI) to interact with **DIRECT** is shown in Figure 2.1. The user is provided with a graphical representation of the shuttle and its cargo bay. A top view and a side view are provided. There are also four functional buttons on this interface. The "Input File" button allows the user to select an input file that has previously been produced. Figure 2.2 shows the interface window that is provided to allow the user to select such an input file. The user will browse the file structure until the appropriate input file is found and then initiate the "Open" button. The user might want to create a new input file by initiating the "Create File" button. The first window the user will then see is provided in Figure 2.3. The user can then move to the appropriate directory with the tools in the upper bar, select an existing filename in the window, or type in a new filename in the lower bar. The "Save" button is initiated to keep the selection and close the window. If an existing filename is used, the user will be prompted for permission to overwrite.

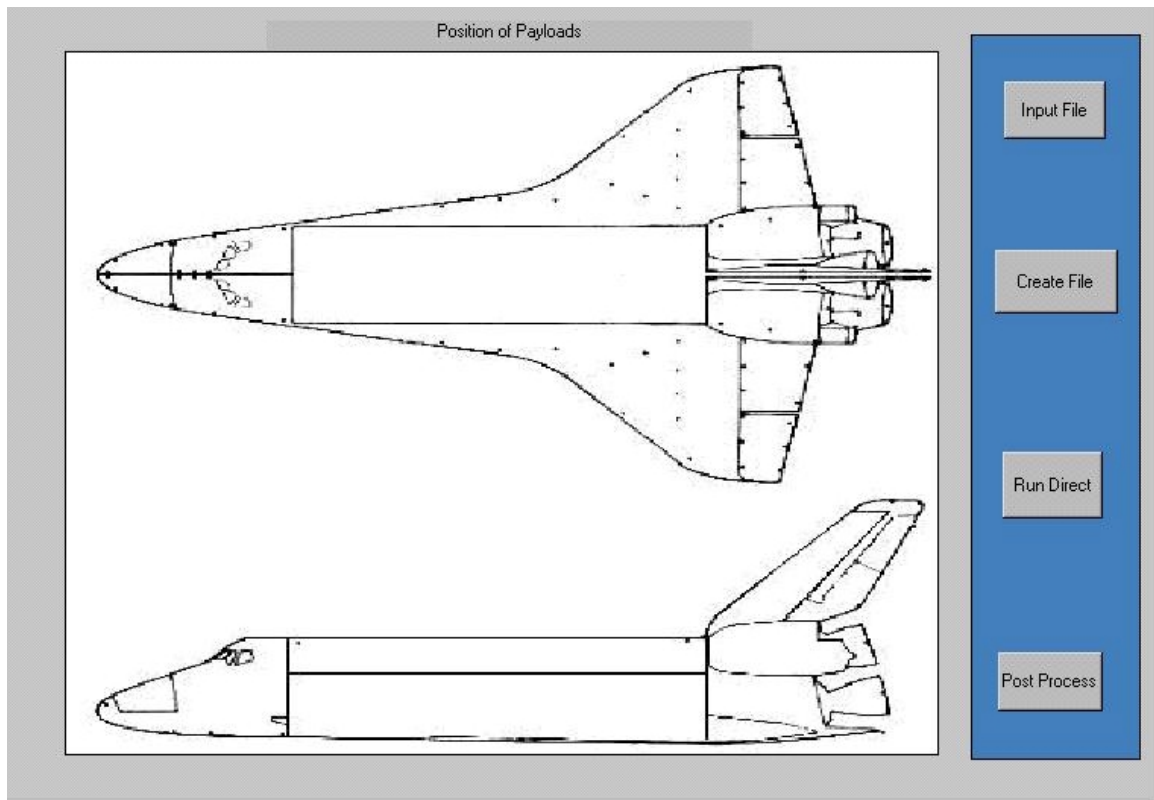


Figure 2.1 Top-Level Interface for **DIRECT**

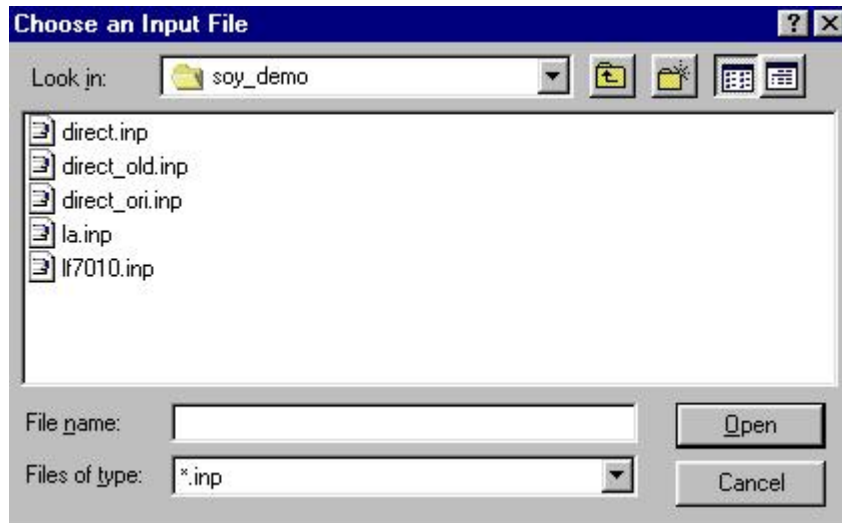


Figure 2.2 Interface Window to Select an Existing **DIRECT** Input File

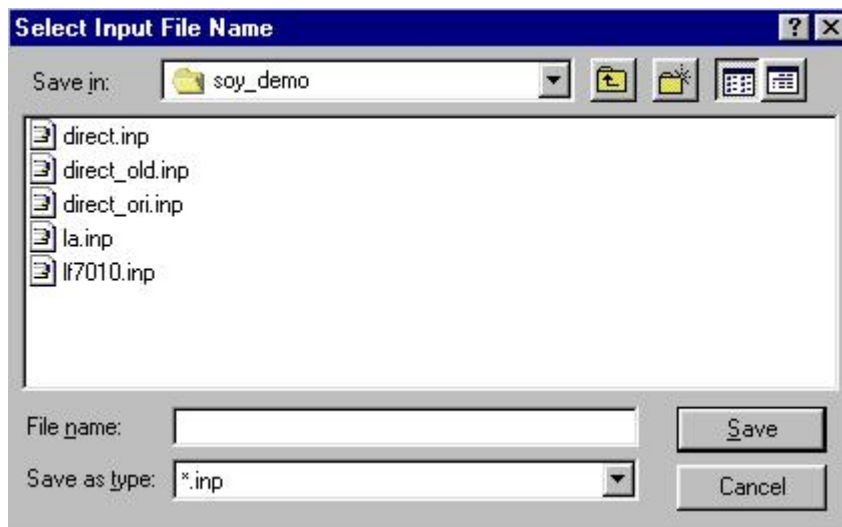


Figure 2.3 Interface Window to Select a Filename for a New **DIRECT** Input File

The next step in creating an input file is to select the output filename. The user is provided with an interface as shown in Figure 2.4 for this selection. The user defines the name for an output file that will contain information useful for debugging the ensuing **DIRECT** run. The next section will discuss the contents of this file in more detail. This file usually has a “.out” extension. The user is then requested to input a filename for an additional output file with a “.mif” extension. This file will contain detailed information of the resulting interface forces. Figure 2.5 shows the interface provided to select this filename.

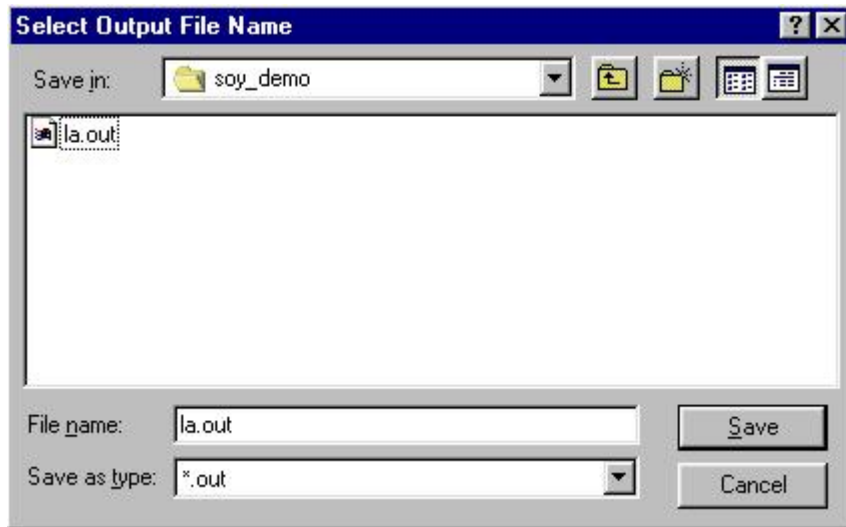


Figure 2.4 Interface Window to Select a **DIRECT** Output File

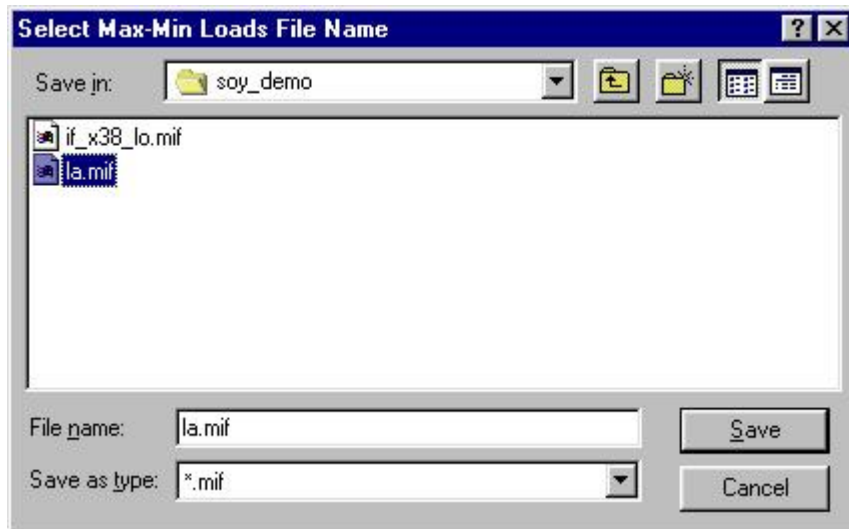


Figure 2.5 Window to Select a **DIRECT** Interface Forces Output Filename

The next step is the selection of the orbiter math model. This is the general description of the Space Shuttle Orbiter with physical descriptions for the payload attach points. Figure 2.6 shows the interface window provided to make this selection. The math model usually ends in ".km". The information provided in this model includes the stiffness and inertia relationships at and between the physical locations for payload attach locations and for the entire Orbiter. Another input file needed to run **DIRECT** is the Degree of Freedom (DOF) map. Like the orbiter model, this file is typically provided to the user by the owner of the primary structure which, in this case, is the Space Shuttle Orbiter. This file contains information that relates the interface nodes of the math model to physical locations in the Orbiter coordinate system. An example of this file is provided in the example section of this manual. The file (which usually has a ".map" extension) is selected using an interface window such as that seen in Figure 2.7.

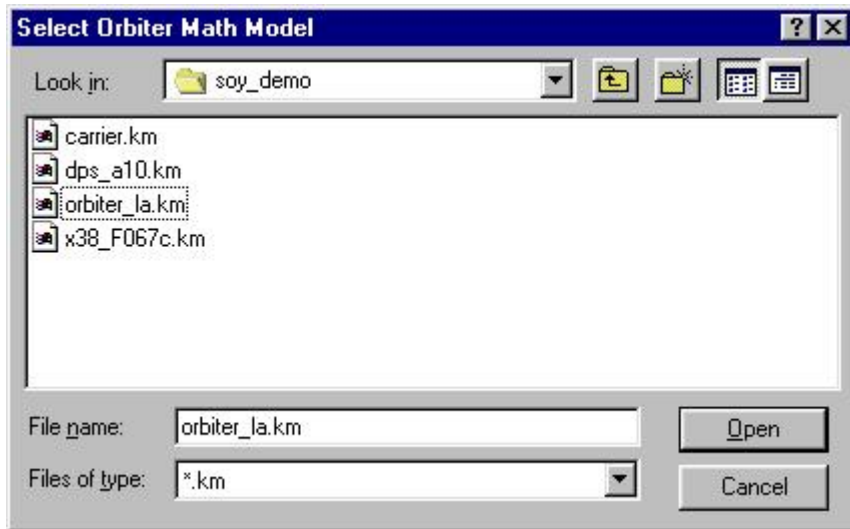


Figure 2.6 Window to Select the Orbiter Math Model for **DIRECT**

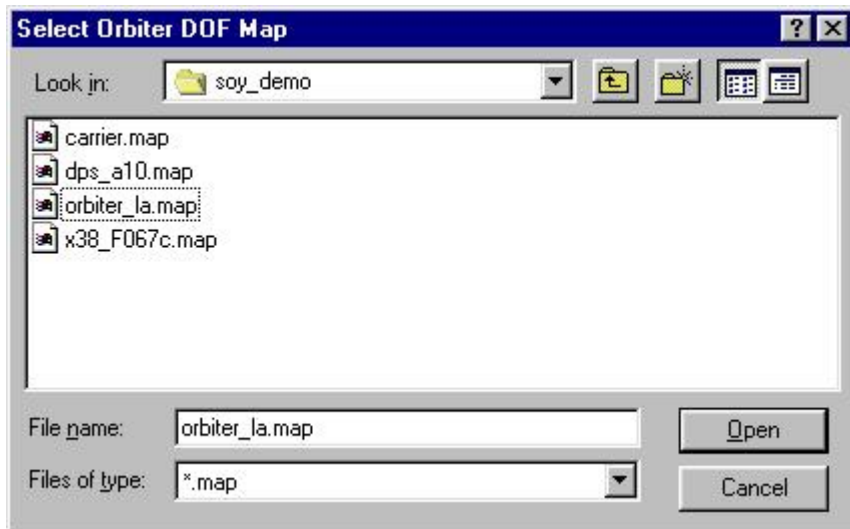


Figure 2.7 Window to Select the Orbiter DOF Map for **DIRECT**

One step in a **DIRECT** run involves the estimation of coupled modes. These modes represent an efficient method to describe the response of a structure. However, if the same model is used repetively for a number of runs, coupled modes do not have to be recalculated. The user is provided with an interface window as shown in Figure 2.8 to input the status of the coupled modes for the orbiter/payload system. The user will activate “Yes” if coupled modes exist and do not need to be recalculated. If this is the status, then the user is provided with a window similar to that seen in Figure 2.9 to locate the appropriate file (which usually ends in “.phi”). If coupled modes need to be recalculated, the user initiates the “No” button in the Figure 2.8 window. A selection window is then provided for the user to select the name of the file.

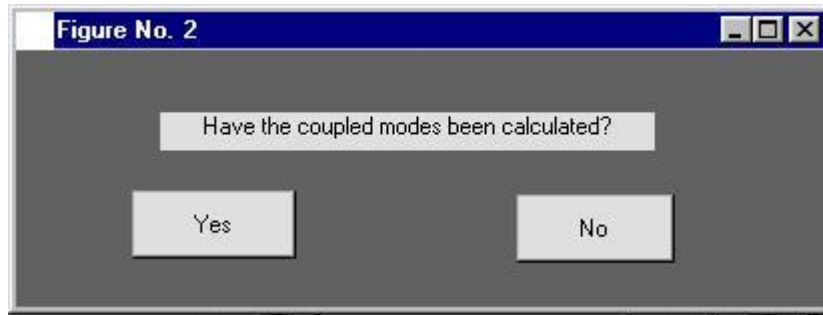


Figure 2.8 Interface Window to Query User about **DIRECT** Coupled Modes

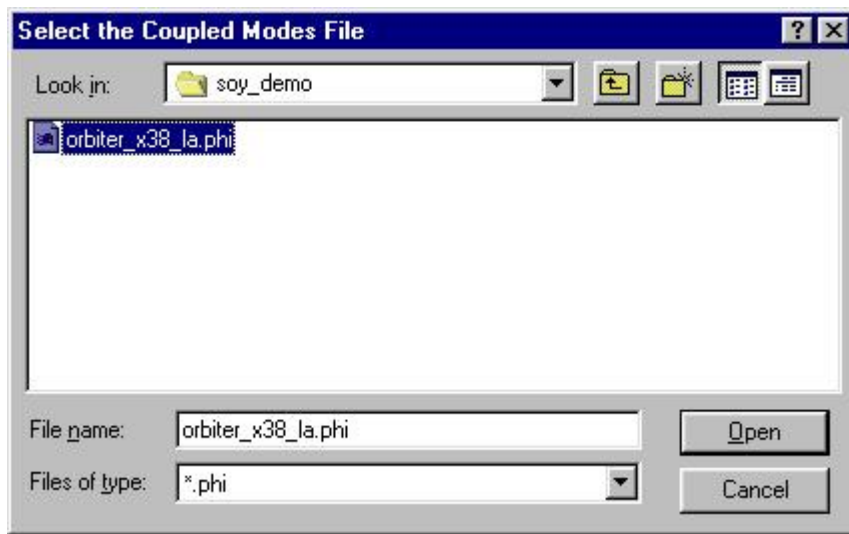


Figure 2.9 Interface Window to Select File Containing **DIRECT** Coupled Modes

The next set of parameters which need to be provided to **DIRECT** include the calculation time step size, number of calculation time steps, and analysis cut-off frequency. **DIRECT** calculations are provided at discrete time steps. The quality of analysis and length of the analysis are determined by these parameters. The Example section provided suggested values for these parameters. The analysis cut-off frequency allows the user to define the vibration frequencies to be included in the analysis. Figures 2.10, 2.11, and 2.12 are replicas of the windows used to provide these parameters. The user will click on the text box with the mouse to activate each window. Then the appropriate value is input using the keyboard. The user will then hit "Enter" to accept the value and continue to the next step.

The user is then ready to designate the payloads to be used. An interface window similar to Figure 2.13 is provided to the user to select the payload math model. This file (which usually has a ".km" extension) contains all the stiffness and inertia information for the payload. Typically, the payload developer provides this model. The developer also provides a payload DOF map that relates the interface DOF's to physical locations in the Orbiter coordinate system. This allows the payload to be connected to the Orbiter model at the proper locations. In fact, a representation of the payload will appear on the Orbiter schematics shown in Figure 2.1. Figure 2.14 provides an interface window used to provide this filename. The user also needs to define a short name for the payload in a window similar to Figure 2.15.

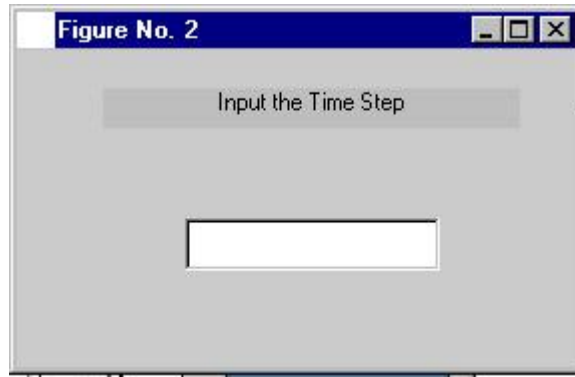


Figure 2.10 Interface For Designating the Time Step Size to be Used in **DIRECT**

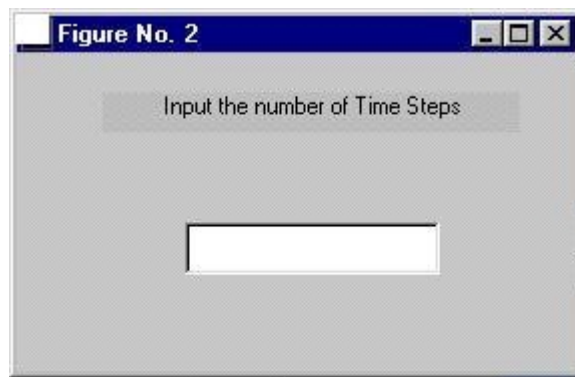


Figure 2.11 Interface for Designating the Number of Time Steps to be Used in **DIRECT**

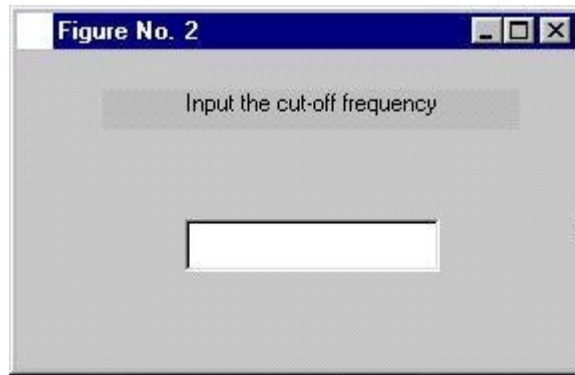


Figure 2.12 Interface for Designating the Maximum Cut-Off Frequency for **DIRECT**

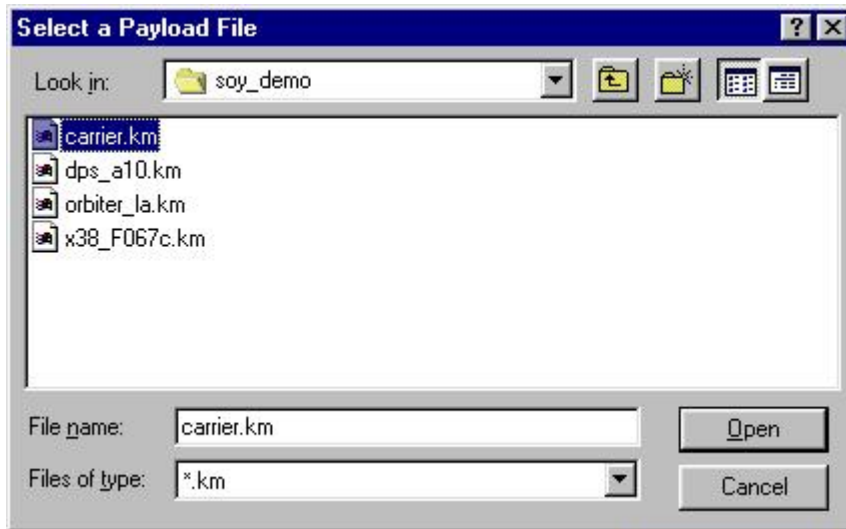


Figure 2.13 Interface to Select a Payload Math Model for **DIRECT**

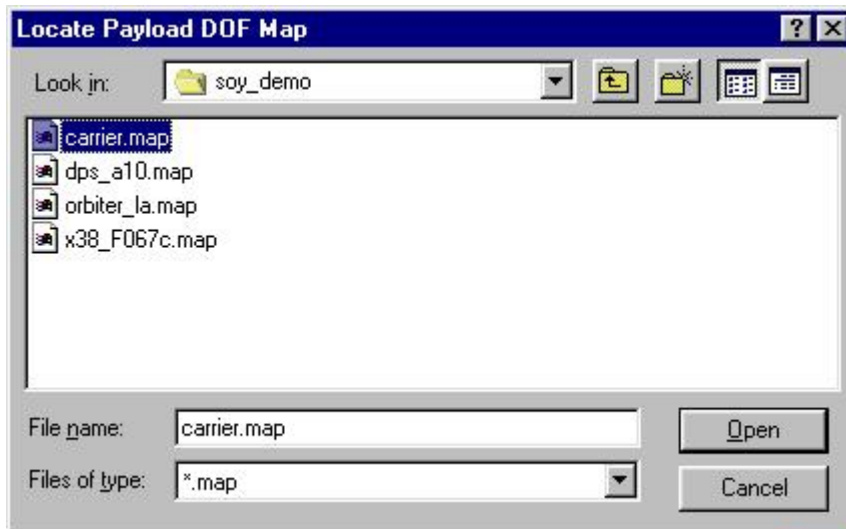


Figure 2.14 Interface to Select a Payload DOF Map for **DIRECT**

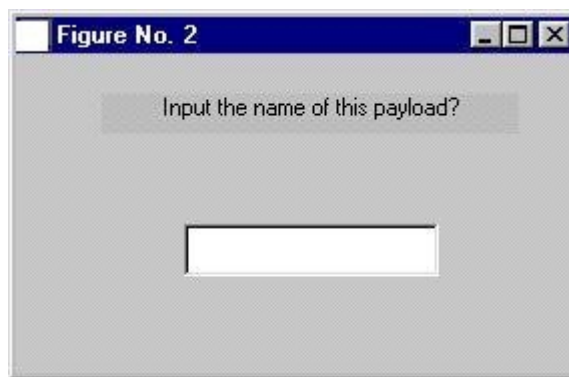


Figure 2.15 Interface to Define the Payload Name for **DIRECT**

The user is given the opportunity to add another payload if desired. If a “Yes” is answered in Figure 2.16, then the user is returned to the window shown in Figure 2.13 to input the next payload. The same loop of Figures 2.13, 2.14, 2.15, and 2.16 is repeated until a “No” input in Figure 2.16 is received. At that point the user is requested to enter the damping parameters for the run. A pair of interface windows similar to that seen in Figure 2.17 is provided. The user enters the damping desired for modes below 10 Hz and a second damping ratio for modes above 10 Hz.

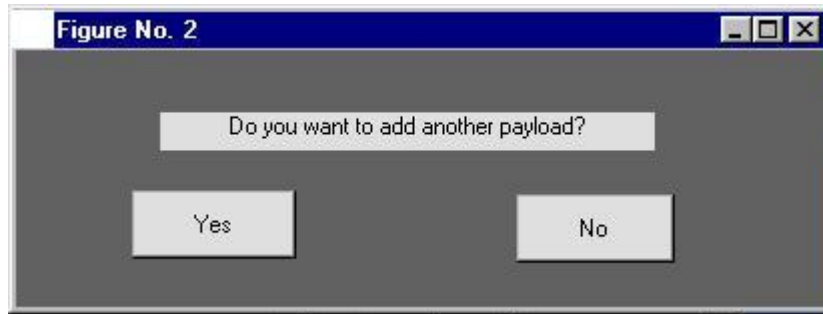


Figure 2.16 Query Window to Select Another Payload for **DIRECT**

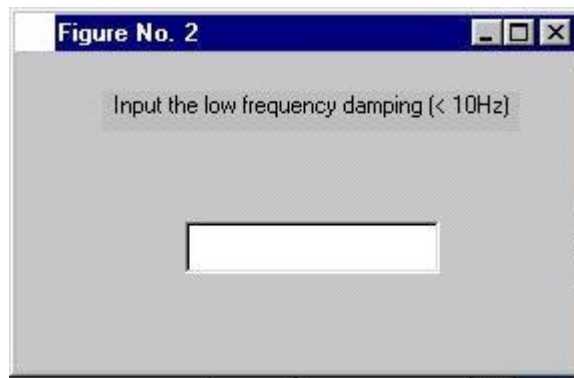


Figure 2.17 Text Input Window to Input Damping into **DIRECT** (1 of 2)

The user is then provided a yes/no query window to select a liftoff run. If the user selects a liftoff run, then a window similar to Figure 2.18 is provided. The user selects from among the 12 liftoff forcing functions. The user selects from the 12 options by a mouse-click in the small boxes. The “Accept” button closes the window and retains the functions selected. Alternatively, the “All” button takes all functions and closes the window. If the user has answered “No” to the liftoff query, then it is assumed that a landing analysis is desired. The user is then provided with Figure 2.19 to select the general cases to run. After selecting the general cases to run, the user is provided with a window similar to Figure 2.20 that is appropriate for each general case selected. Hence if all general cases were selected, then six versions of Figure 2.20 would be provided. Figures 2.21 and 2.22 are then provided to the user to select the center of gravity location and landing configuration. The selected options for these parameters will be applied to each landing test case previously selected. After all selections are made an input file similar to that shown in Figure 2.23 is produced. Obviously, the user can edit a file outside of the user interface to make simple modifications.

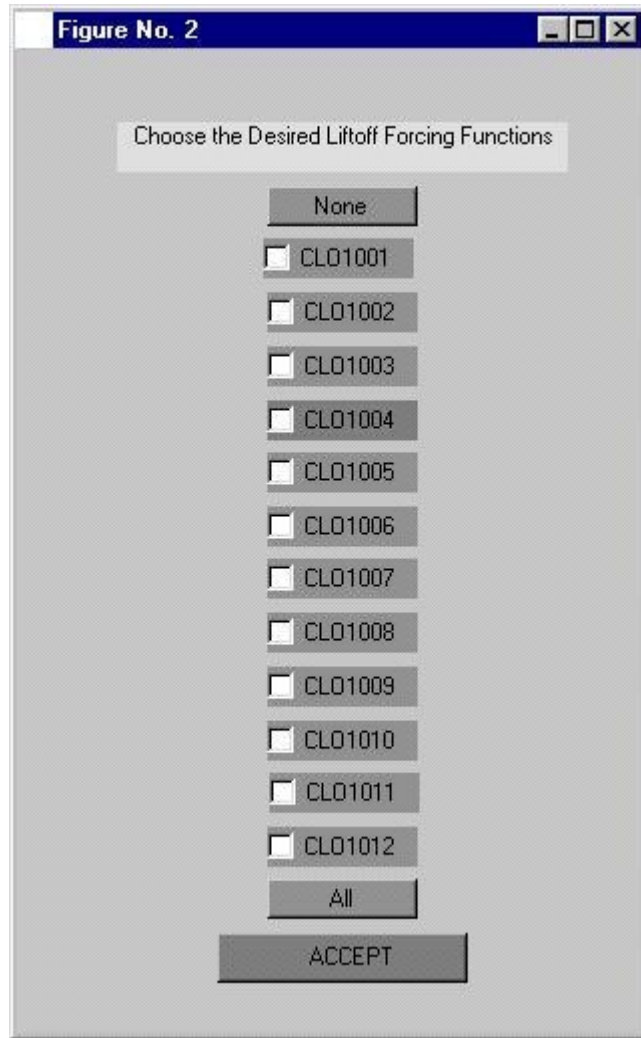


Figure 2.18 Liftoff Forcing Function Selection for **DIRECT**

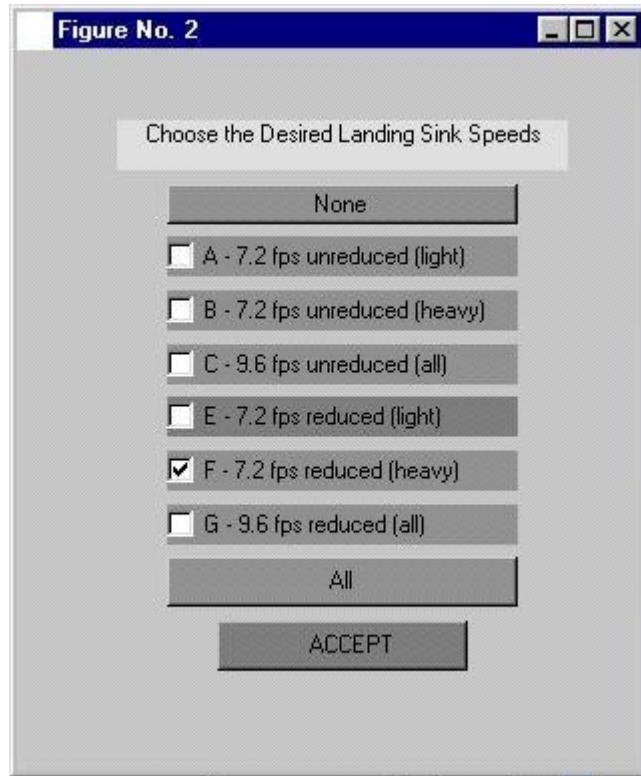


Figure 2.19 General Landing Case Selection Window

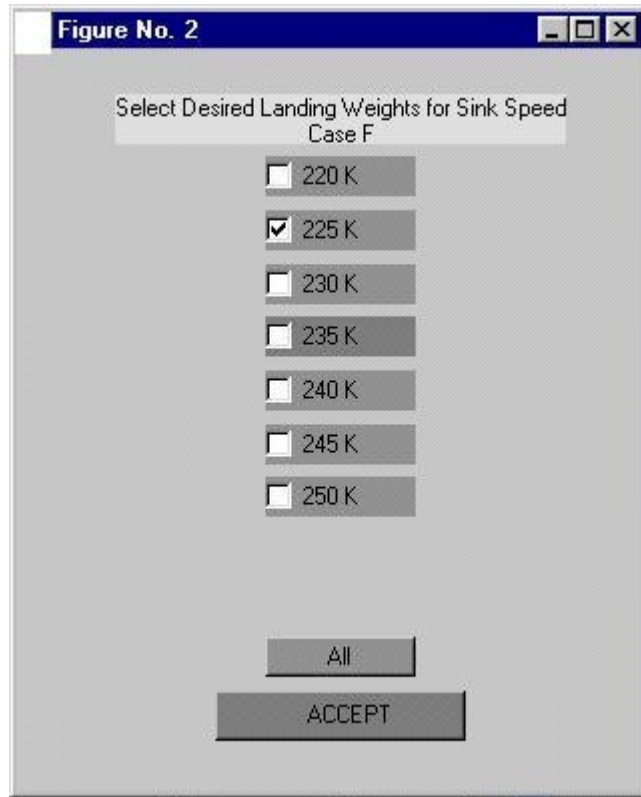


Figure 2.20 Landing Weight Selection Window (1 of 6)

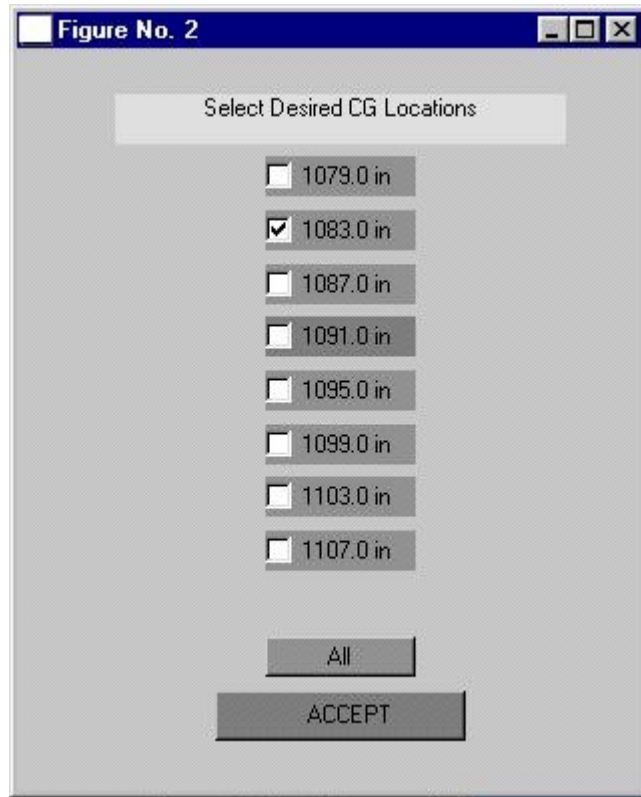


Figure 2.21 Center of Gravity Selection Window

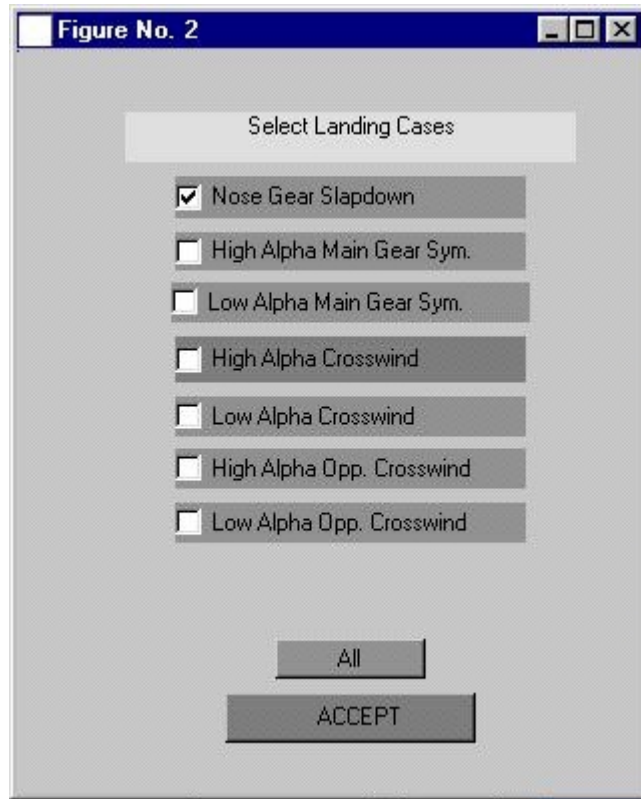
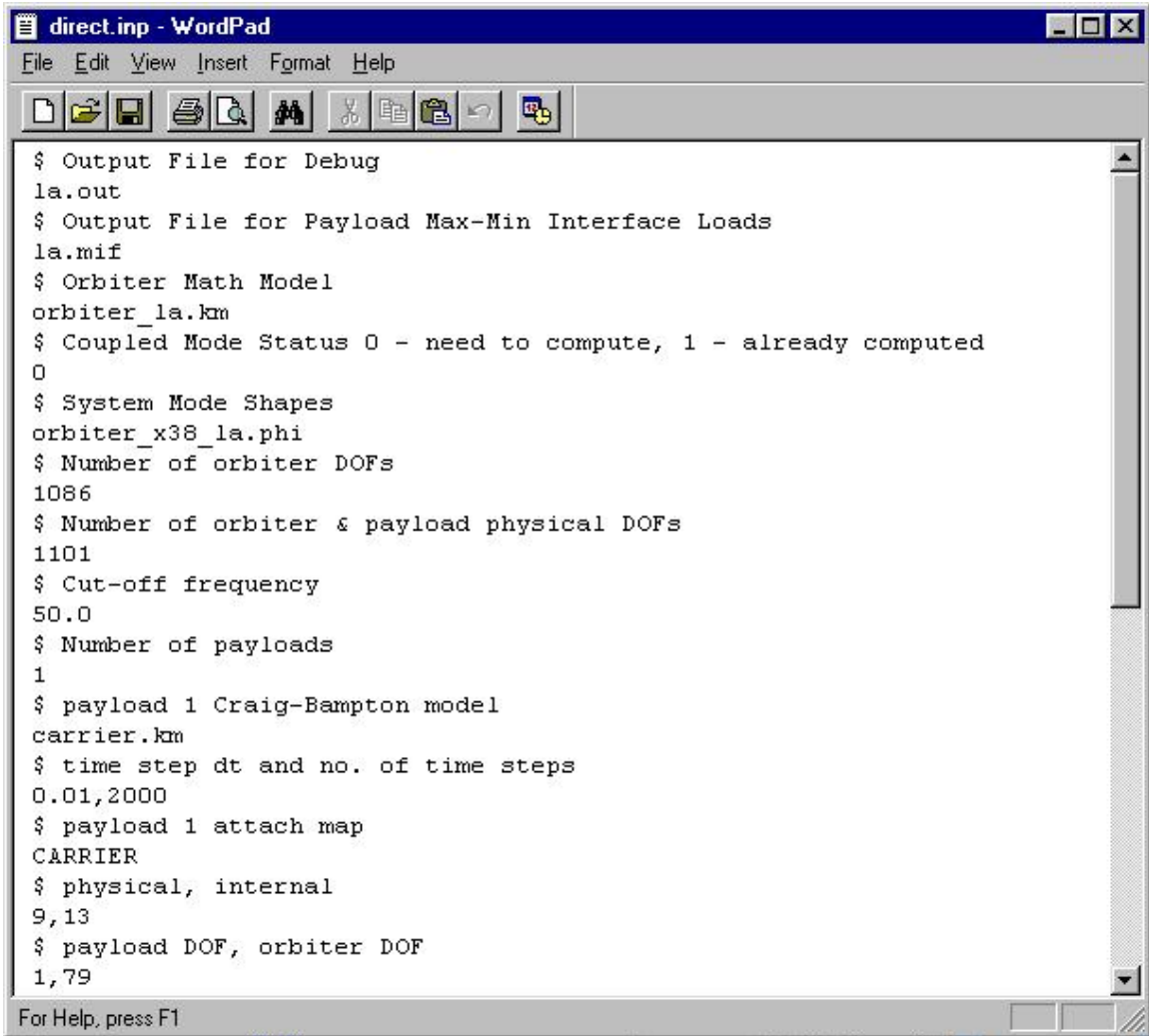


Figure 2.22 Landing Configuration Selection Window



```
$ Output File for Debug
la.out
$ Output File for Payload Max-Min Interface Loads
la.mif
$ Orbiter Math Model
orbiter_la.km
$ Coupled Mode Status 0 - need to compute, 1 - already computed
0
$ System Mode Shapes
orbiter_x38_la.phi
$ Number of orbiter DOFs
1086
$ Number of orbiter & payload physical DOFs
1101
$ Cut-off frequency
50.0
$ Number of payloads
1
$ payload 1 Craig-Bampton model
carrier.km
$ time step dt and no. of time steps
0.01,2000
$ payload 1 attach map
CARRIER
$ physical, internal
9,13
$ payload DOF, orbiter DOF
1,79

For Help, press F1
```

Figure 2.23 Example of **DIRECT** Input File Produced

The “Run Direct” button on Figure 2.1 actually performs a **DIRECT** run using the last file create, the last file selected, or the current file named “direct.inp”.

3. DIRECT OUTPUT

For each forcing function and each payload, output data are written to the following files

Lf7010_carrier.mif - Summary of max-min payload interface forces

Lf7010_carrier.mdi - Summary of max-min payload interface displacements

Lf7010_carrier.mac - Summary of max-min payload interface acceleration

Lf7010_carrier.if - Time histories of the payload interface forces

Lf7010_carrier.dis - Time histories of the payload displacements

Lf7010_carrier.acc - Time histories of the payload accelerations

In addition, a summary of the payload maximum-minimum interface forces due to all the forcing functions are written. An example of this output is shown in Figure 3.1.

The screenshot shows a WordPad window titled 'if_x38_lo.mif - WordPad'. The text content is as follows:

```

DPS MODEL
MAX MIN INTERAFCE FORCE

Grid      Description      TIME sec.  MIN I/F lbs.  FF      TIME sec.  MAX I/F lbs.  FF
80001    DX3 Y28 UP PORT  X-DIR      8.680     -20376.799 1r5129v  3.980     2505.676 1r5123v
          Y-DIR      3.982      -226.802 1r5123v  7.028     13004.185 1r5123v
          Z-DIR      7.150     -1884.913 1r5123v  7.054      7868.382 1r5123v
80002    DX4 Y28 UP STBD X-DIR      7.490     -21089.527 1r5123v  7.144     3020.323 1r5123v
          Y-DIR      7.018     -11918.507 1r5123v  7.130      776.894 1r5123v
          Z-DIR      7.150     -1729.032 1r5123v  7.048     8515.536 1r5123v
80003    DX1 Z37 PORT    X-DIR      7.018     -47806.449 1r5123v  3.970     1218.976 1r5123v
          Y-DIR      3.972      487.200 1r5123v  7.020     17466.867 1r5123v
          Z-DIR      7.018     -12311.203 1r5123v  3.970     -708.626 1r5123v
80004    DX5 Y28 PORT    X-DIR      7.132     -2381.320 1r5123v  7.042     27060.504 1r5123v
          Y-DIR      7.130      -402.348 1r5123v  7.020     16043.383 1r5123v
          Z-DIR      7.144     -683.143 1r5123v  7.482     2737.579 1r5123v
80005    DX6 Y28 PORT    X-DIR      3.978     -1442.202 1r5123v  7.040     26013.096 1r5123v
          Y-DIR      7.020     -16820.111 1r5123v  7.132     -466.450 1r5123v
          Z-DIR      5.362     -258.454 1r5129v  7.042     3502.842 1r5123v
80006    DX2 Z37 STBD   X-DIR      7.022     -47403.340 1r5123v  7.130     -1019.352 1r5123v
          Y-DIR      7.022     -17511.723 1r5123v  7.130     -1335.864 1r5123v
          Z-DIR      7.022     -12216.131 1r5123v  4.694     -1008.947 1r5129v
81188    DPS/ORB PORT    X-DIR      3.972     -1708.498 1r5123v  7.020     45983.773 1r5123v
          Z-DIR      6.930     -13292.397 1r5123v  6.902     13663.006 1r5123v
81197    DPS/ORB KEEL   Y-DIR      8.678     -14348.574 1r5129v  8.320     13141.765 1r5129v
  
```

Figure 3.1 Payload Interface Force Max-Min Summary

In addition, the time histories of data from DIRECT are written in spread sheet format. Any commercial plotting software can be used for viewing these data. An interface force time history is shown in Figure 3.2.

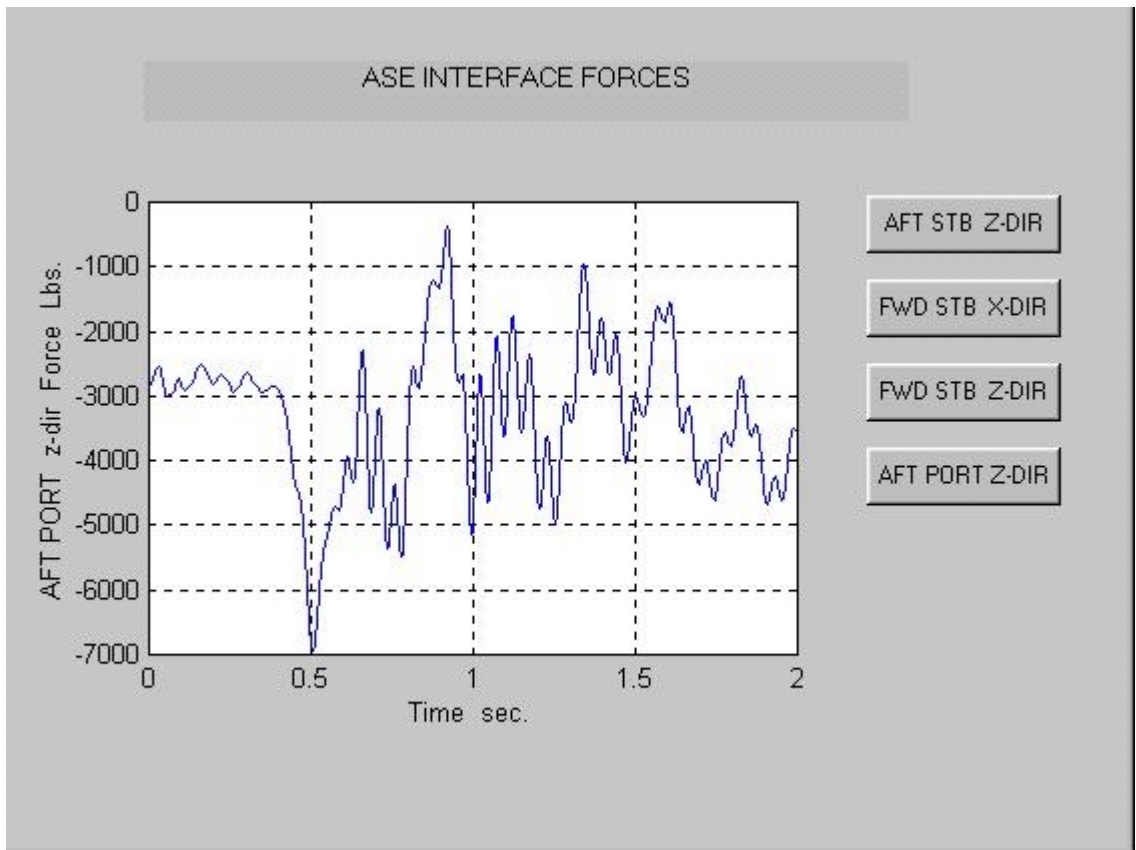


Figure 3.2 Interface Force Time History

4. EXAMPLE

4.1 Input Data

This section provides example data files for **DIRECT**. In this example, a landing simulation of the orbiter with three payloads are used for illustration of **DIRECT** simulation.

Orbiter math model files:

Orbiter_la.km - Math model file

Orbiter_la.map - Model geometry file

Payload 1 : Carrier

Carrier.km

Carrier.map

Payload 2: De-orbit Propulsion System

Dps.km

Dps.map

Payload 3: X38 Crew Return Vehicle

X38.km

X38.map

Forcing Functions: lf7010 and lf7011

Example of format of geometry file is shown in Table 4.1

Table 4.1 Payload Geometry Input

2990 Aft STBD	852.670	94.000	414.000	0	0	1	0	0	0
2991 FWD STBD	793.670	94.000	414.000	2	0	3	0	0	0
4291 X38/ASE STBD	818.850	32.844	391.750	0	0	4	0	0	0
3283 KEEL	825.130	0.000	305.000	0	5	0	0	0	0
4773 X38/ASE PORT	818.850	-32.844	391.750	0	0	6	0	0	0
6814 FWD PORT	793.670	-94.000	414.000	7	0	8	0	0	0
6813 AFT PORT	852.670	-94.000	414.000	0	0	9	0	0	0

Example of input file for **DIRECT** is presented in Table 4.2

Table 4.2 Input data for Example Problem

```
$ OUTPUT FILE FOR DEBUG
landing.out
$ OUTPUT FILE FOR PAYLOAD MAX-MIN INTERFACE LOADS
landing.mif
$ orbiter math model
orbiter_la.km
$ coupled mode status 0 - need to compute. 1 - already computed
0
$ system mode shapes
orb_la.phi
$ no. of orbiter 1 DOF
1086
$ no. of orbiter physical DOF + PAY
1423
$ cut-off freq
50.0
$ no. of payload
3
$ payload 1 model
carrier.km
$ payload 2 model
x38.km
$ payload 3 model
dps.km
$ time step dt and no. of time step
.001,2000
$ payload 1 attach map
ASE CARRIER (LA)
$ physical, internal
9,13
$ payload DOF, ORBITER DOF
1,79
2,71
3,73
4,1087
5,90
6,1088
7,74
8,76
9,82
10,1089
2990   AFT      STBD   Z-DIR
2991   FWD     STBD   X-DIR
       Z-DIR
4291   X38/ASE  STBD   Z-DIR
3283   KEEL                    Y-DIR
4773   X38/ASE  PORT   Z-DIR
6814   FWD     PORT   X-DIR
```

```

                                Z-DIR
6813   AFT      PORT  Z-DIR
$ payload 2 attach map
X38 MODEL
$ physical, internal
20,257
$ payload DOF, ORBITER DOF
1,1088
2,1087
3,1102
4,1103
5,1104
6,1105
7,1106
8,1107
9,1108
10,1109
11,1110
12,1111
13,1112
14,1113
15,1114
16,1115
17,1116
18,1117
19,1118
20,1119
21,1120
17301  ASE I/F  PORT  Z-DIR
17302  ASE I/F  STBD  Z-DIR
150403  DX1 Z37  PORT  X-DIR
                                Y-DIR
                                Z-DIR
150406  DX2 Z37  STBD  X-DIR
                                Y-DIR
                                Z-DIR
150401  DX3 Y28  UP  PORT  X-DIR
                                Y-DIR
                                Z-DIR
150402  DX4 Y28  UP  STBD  X-DIR
                                Y-DIR
                                Z-DIR
150405  DX6 Y28  PORT  X-DIR
                                Y-DIR
                                Z-DIR
150404  DX5 Y28  PORT  X-DIR
                                Y-DIR
                                Z-DIR

$ payload 3 attach map
DPS MODEL
$ physical, internal
23,47
$ payload DOF, ORBITER DOF
1,1108
2,1109
3,1110
4,1111

```


4.2 Output Data

The max-min interface forces of three payloads are shown in Table 4.2. The time history of the interface load for the carrier due to lf7010 force is plotted in Figure 4.1

Table 4.2 Payload Interface Force Summary

ASE CARRIER (LA)				MIN		MAX	
MAX MIN INTERFACE FORCE							
2990	AFT	STBD	Z-DIR	0.228	-9329.968	lf7011	0.631 431.418 lf7011
2991	FWD	STBD	X-DIR	0.224	-740.070	lf7011	0.282 1091.692 lf7011
			Z-DIR	0.068	-12047.791	lf7011	0.635 -70.560 lf7011
4291	X38/ASE	STBD	Z-DIR	0.633	-574.369	lf7011	0.067 18716.361 lf7011
3283	KEEL		Y-DIR	1.424	-2629.237	lf7010	1.232 2745.611 lf7010
4773	X38/ASE	PORT	Z-DIR	0.631	-530.905	lf7011	0.068 19175.578 lf7011
6814	FWD	PORT	X-DIR	0.344	-726.113	lf7011	0.280 1186.797 lf7011
			Z-DIR	0.068	-12114.760	lf7011	0.634 44.930 lf7011
6813	AFT	PORT	Z-DIR	0.229	-9344.721	lf7011	0.631 474.847 lf7011
X38 MODEL				MIN		MAX	
MAX MIN INTERFACE FORCE							
17301	ASE I/F	PORT	Z-DIR	0.068	-19216.051	lf7011	0.631 620.857 lf7011
17302	ASE I/F	STBD	Z-DIR	0.067	-18732.610	lf7011	0.632 734.419 lf7011
150403	DX1 Z37	PORT	X-DIR	0.509	-15536.635	lf7011	0.337 9489.246 lf7011
			Y-DIR	0.337	-5050.506	lf7011	0.510 7580.915 lf7011
			Z-DIR	0.510	-7815.852	lf7011	0.336 5109.821 lf7011
150406	DX2 Z37	STBD	X-DIR	0.603	-16087.642	lf7010	0.339 10036.041 lf7011
			Y-DIR	0.510	-7176.160	lf7011	0.335 4802.607 lf7011
			Z-DIR	0.510	-7624.923	lf7011	0.335 4999.599 lf7011
150401	DX3 Y28	UP PORT	X-DIR	0.618	-969.176	lf7011	0.226 17264.725 lf7011
			Y-DIR	0.200	-10090.916	lf7011	0.437 2039.220 lf7010
			Z-DIR	0.197	-7571.158	lf7011	0.615 772.682 lf7011
150402	DX4 Y28	UP STBD	X-DIR	0.617	-1654.614	lf7011	0.307 16864.768 lf7011
			Y-DIR	0.438	-2035.622	lf7010	0.199 10256.267 lf7011
			Z-DIR	0.195	-7800.954	lf7011	0.615 873.190 lf7011
150405	DX6 Y28	PORT	X-DIR	0.195	-14252.417	lf7011	0.145 3979.910 lf7011
			Y-DIR	0.145	-791.742	lf7011	0.313 3745.759 lf7011
			Z-DIR	0.192	-3613.160	lf7011	0.145 616.412 lf7011
150404	DX5 Y28	PORT	X-DIR	0.195	-14274.559	lf7011	0.145 4032.059 lf7011
			Y-DIR	0.193	-3790.832	lf7011	0.144 753.728 lf7011
			Z-DIR	0.193	-3591.470	lf7011	0.145 675.600 lf7011
DPS MODEL				MIN		MAX	
MAX MIN INTERFACE FORCE							
80001	DX3 Y28	UP PORT	X-DIR	0.225	-15853.039	lf7011	0.901 1749.547 lf7010
			Y-DIR	0.141	-1548.815	lf7011	0.198 10339.982 lf7011
			Z-DIR	0.842	-893.703	lf7010	0.215 7438.172 lf7011
80002	DX4 Y28	UP STBD	X-DIR	0.224	-15383.605	lf7011	0.617 1800.439 lf7011
			Y-DIR	0.197	-10322.095	lf7011	0.141 1756.659 lf7011
			Z-DIR	0.908	-1074.341	lf7010	0.313 7477.825 lf7011
80003	DX1 Z37	PORT	X-DIR	0.337	-10759.307	lf7011	0.509 15414.103 lf7011
			Y-DIR	0.510	-7648.116	lf7011	0.336 5143.026 lf7011
			Z-DIR	0.336	-4633.121	lf7011	0.510 8448.737 lf7011
80004	DX5 Y28	PORT	X-DIR	0.144	-3735.739	lf7011	0.195 13954.775 lf7011
			Y-DIR	1.099	-1485.800	lf7010	0.195 3157.764 lf7011
			Z-DIR	0.143	-657.860	lf7011	0.195 3068.784 lf7011
80005	DX6 Y28	PORT	X-DIR	0.144	-3706.846	lf7011	0.195 13912.701 lf7011
			Y-DIR	0.312	-3239.915	lf7011	0.688 1471.371 lf7010
			Z-DIR	0.144	-620.347	lf7011	0.194 3039.108 lf7011
80006	DX2 Z37	STBD	X-DIR	0.339	-11269.940	lf7011	0.510 15759.110 lf7011
			Y-DIR	0.335	-4950.166	lf7011	0.510 7336.737 lf7011
			Z-DIR	0.334	-4774.116	lf7011	0.510 8174.607 lf7011
81459	DPS/ORB	PORT	X-DIR	0.510	-10551.651	lf7011	0.334 13895.819 lf7011
			Z-DIR	0.226	-22915.509	lf7011	0.905 3045.162 lf7010

81484	DPS/ORB	KEEL	Y-DIR	0.554	-3215.999	lf7011	0.507	3569.004	lf7011
81489	DPS/ORB	STBD	X-DIR	0.511	-9525.359	lf7011	0.335	13385.528	lf7011
			Z-DIR	0.292	-23034.194	lf7011	0.632	2269.988	lf7010

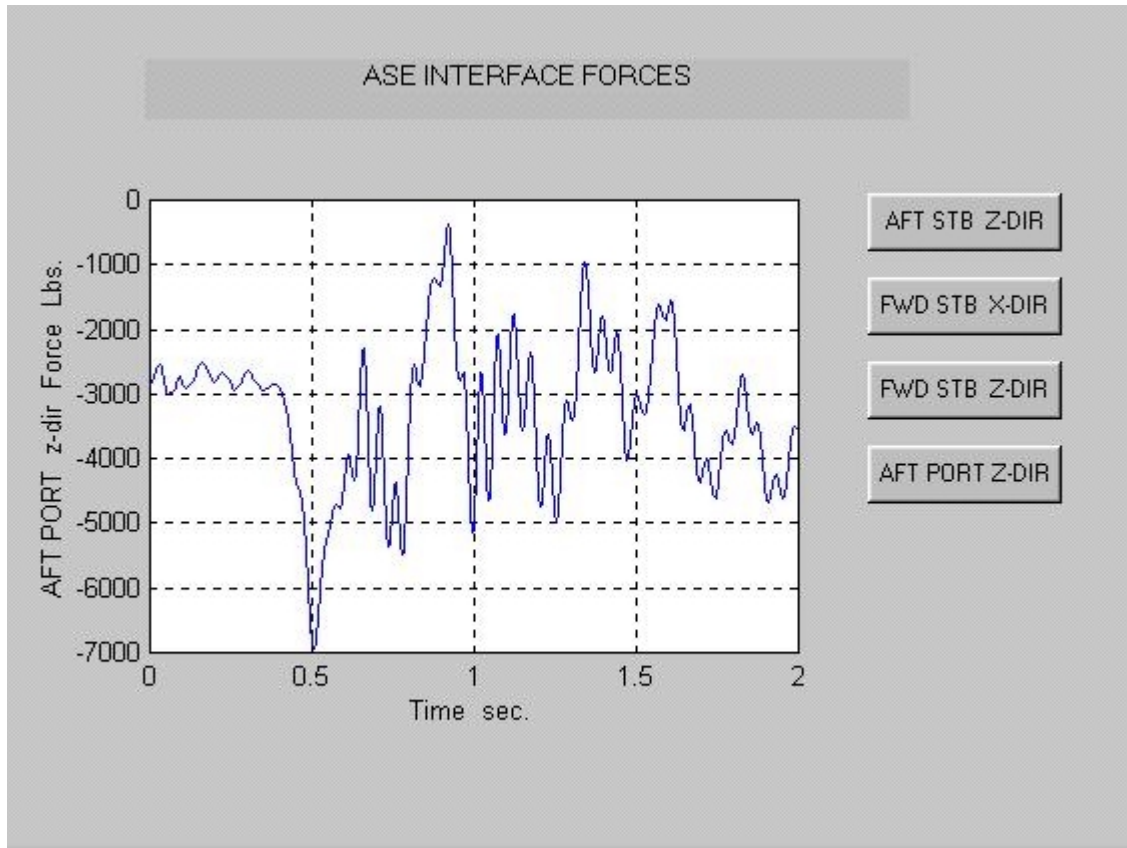


Figure 4.1 Carrier Interface Force for lf7001

5. DIRECT MATHEMATICAL BACKGROUND

5.1 Introduction

In this chapter, several mathematical and structural analysis techniques that will be used throughout the remaining chapters will be discussed. In section 2.2, the normal mode analysis is presented. Structural engineers frequently use two products of normal mode analysis for analytical model validation and structural damage detection, namely natural frequencies and mode shapes. The mathematical derivation of Ritz vectors is described in section 2.3. Finally, several techniques frequently used in FE modal validation and structural damage detection are briefly presented.

5.2 Normal Mode Analysis

Normal mode analysis has been used extensively in the area of structural dynamics. For many years, structural engineers have been using numerical techniques based on normal mode analysis to determine resonant frequencies (eigenvalues) of complex structural systems for safety concerns. In addition, normal mode shapes (eigenvectors) have been utilized to simplify the transient response analysis process of large complex structural systems. Typically, the large set equation of motion represent the structure system are decoupled into a limited number of normal mode coordinates. This section will give a brief overview of normal mode analysis.

5.2.1 Normal Mode Analysis of Undamped Systems

For an undamped multi-degree-of-freedom system, the governing equations of motion can be expressed as

$$M\ddot{x} + Kx = B_0 u(t), \quad (5.1)$$

where M and K are the $n \times n$ analytical mass and stiffness matrices, x is an $n \times 1$ vector of position, B_0 is the $n \times m$ actuator influence matrix, $u(t)$ is the $m \times 1$ vector of applied forces, and the overdots represent differentiation with respect to time.

In order to determine the free vibration solution, the applied force can be set to zero. The homogenous solution for Equation (5.1) can be assumed as

$$x(t) = \Psi e^{j\omega t}. \quad (5.2)$$

Substituting Equation (5.2) into Equation (5.1) yield the undamped eigenproblem,

$$(K - \omega^2 M)\Psi e^{j\omega t} = 0, \quad (5.3)$$

for which the non-trivial solution is defined by

$$\det(K - \omega^2 M) = 0. \quad (5.4)$$

Equation (5.4) is a n^{th} order polynomial in (ω^2) with real coefficients. Thus, there will be n roots; $(\omega_1^2, \omega_2^2, \dots, \omega_r^2, \dots, \omega_n^2)$. These roots are the undamped system natural frequencies. Substituting any of these natural frequencies into Equation (5.3) yields a corresponding set of relative values of Ψ_r . The vector Ψ_r is called the r^{th} mode shape corresponding to the r^{th} natural frequency.

The most important property of mode shapes is the orthogonality property. It can be expressed as

$$\Psi^T M \Psi = [m]$$

and (5.5)

$$\Psi^T K \Psi = [k],$$

where $[m]$ and $[k]$ are diagonal matrices often referred as the modal mass and stiffness. The values of modal mass and stiffness of modes are not unique. Among the many scaling or normalization processes, there is one which has the most relevance to modal testing and that is mass normalization. The mass normalized mode shape Φ have the following particular property

$$\Phi^T M \Phi = [I]$$

and (5.6)

$$\Phi^T K \Phi = [\omega^2].$$

The relationship between the mass normalized mode shape for mode r^{th} , Φ_r and its more general form Ψ_r is

$$\Phi_r = \frac{1}{\sqrt{m_r}} \Psi_r. \quad (5.7)$$

Using the mass normalized property, a change of basis can be defined as

$$x(t) = \Phi q(t). \quad (5.8)$$

Applying the transformation in Equation (5.8) to Equation (5.1), the governing equations of motion can be written as

$$\ddot{q}_i + \omega_i^2 q_i = \Phi_i^T f(t), \text{ where } i = 1, 2, \dots, n. \quad (5.9)$$

Equation (5.9) represents a set of single DOF equations and can be easily solved.

5.2.2 General Damped Systems

All physical systems possess some level of damping. The equations of motion for damped MDOF systems can be expressed as

$$M\ddot{x} + D\dot{x} + Kx = B_0 u(t), \quad (5.10)$$

where D is the general damping matrix.

Similar to the undamped system, a solution to Equation (5.10) can be assumed as

$$x(t) = \Psi e^{\lambda t}. \quad (5.11)$$

Substituting Equation (5.11) into the damped equations of motion (5.10), and assuming zero forces results in the eigenvalue problem

$$(\lambda^2 M + \lambda D + K)\Psi e^{\lambda t} = 0. \quad (5.12)$$

Equation (5.12) can be recast into a state space representation as

$$\begin{bmatrix} 0 & I \\ -M^{-1}K & -M^{-1}D \end{bmatrix} \begin{Bmatrix} \Psi \\ \lambda \Psi \end{Bmatrix} = \lambda \begin{Bmatrix} \Psi \\ \lambda \Psi \end{Bmatrix}. \quad (5.13)$$

In this case, there are $2n$ eigenvalues and they occur in complex conjugate pairs. To each of these eigenvalues, there is a corresponding eigenvector. These eigenvectors also occur as complex conjugate pair. The eigenvalues or damped frequencies can be written as

$$\lambda_i = \omega_i (-\zeta_i \pm j\sqrt{1-\zeta_i^2}), \quad (5.14)$$

where ω_i is the i^{th} natural frequency of the undamped system and ζ_i is the damping ratio of the i^{th} mode. A pair of the complex conjugate mode shape can be determined as

$$\Psi_i = \Psi_{iR} + j\Psi_{iI}, \quad (5.15)$$

where Ψ_{iR} is the real part of the mode shape and Ψ_{iI} is the imaginary part.

The orthogonality property is more complicated for the general damped system than for the undamped system. One method of normalization of the mode shapes gives

$$\begin{bmatrix} \lambda\Psi & (\lambda\Psi)^* \\ \Psi & \Psi^* \end{bmatrix}^T \begin{bmatrix} 0 & M \\ M & D \end{bmatrix} \begin{bmatrix} \lambda\Psi & (\lambda\Psi)^* \\ \Psi & \Psi^* \end{bmatrix} = [I]$$

and (5.16)

$$\begin{bmatrix} \lambda\Psi & (\lambda\Psi)^* \\ \Psi & \Psi^* \end{bmatrix}^T \begin{bmatrix} -M & 0 \\ 0 & K \end{bmatrix} \begin{bmatrix} \lambda\Psi & (\lambda\Psi)^* \\ \Psi & \Psi^* \end{bmatrix} = \begin{bmatrix} \lambda & \\ & \lambda^* \end{bmatrix},$$

with the superscript * representing the complex conjugate operator.

5.2.3 Proportionally Damped Systems

A special case of damping in which the damping matrix can be transformed into a diagonal matrix is called proportional damping and has the following form

$$D = \beta K + \gamma M, \quad (5.17)$$

where β and γ are real scalars.

In this case, the damped system will have the damped frequencies and mode shapes described as follow

$$\omega_r^d = \omega_r^n \sqrt{1 - \zeta_r^2}; \text{ with } \zeta_r = \frac{\beta\omega_r^n}{2} + \frac{\gamma}{2\omega_r^n},$$

and (5.18)

$$\Psi_{damped} = \Psi_{undamped} \cdot$$

A more general requirement for a damped system to possess the same mode shapes as its undamped counterpart is

$$DM^{-1}K = KM^{-1}D. \quad (5.19)$$

5.3 DIRECT Ritz Vector Computation

The computation of Ritz vectors as defined by Wilson et al. (1982) starts with the static solution of

$$Kv_1^* = B_0u_s, \quad (5.20)$$

where u_s is the static load. The subsequent Ritz vectors are mass normalized. However, this algorithm will result in a diagonal mass matrix and a fully populated stiffness matrix.

In **DIRECT** Ritz vector computation, the Wilson algorithm is modified. The first Ritz vector is obtained by normalizing the static solution vector with respect to the stiffness matrix

$$v_1 = \frac{v_1^*}{(v_1^{*T}Kv_1^*)^{1/2}}. \quad (5.21)$$

The first Ritz vector will be subsequently termed the static Ritz vector. The calculation of subsequent dynamic Ritz vectors begin with the following recurrence relation

$$Kv_i^* = Mv_{i-1}, \quad (5.22)$$

which includes the inertia effects. The vector v_i^* is then stiffness orthogonalized with respect to the previous vectors using the Gram-Schmidt process

$$v_i^{**} = v_i^* - \sum_{j=1}^{i-1} (v_j^T K v_i^*) v_j. \quad (5.23)$$

Finally, the i^{th} dynamic Ritz vector v_i is obtained by normalizing v_i^{**} to satisfy

$$v_i^T K v_i = 1. \quad (5.24)$$

Using the mode superposition method the position vector x in Equation (5.1) can be expressed as

$$x = Vq, \quad (5.25)$$

where V is the $n \times p$ matrix of Ritz vectors and q is the $p \times 1$ unknown time function. Usually, p is much smaller than n . Substituting Equation (5.25) into Equation (5.1) and pre-multiplying by V^T yields

$$M^* \ddot{q} + K^* q = V^T B_0 u(t), \quad (5.26)$$

where

$$M^* = V^T M V \text{ and } K^* = V^T K V. \quad (5.27)$$

The advantage of this algorithm is that M^* is a tri-diagonal matrix and K^* is a diagonal matrix. A comparison of the characteristics of Ritz vectors and normal mode shapes is presented in Table 5.1, which illustrates the advantages of Ritz Vectors.

Table 5.1
Comparison of Characteristics of Ritz Vectors and Normal Mode Shapes

Characteristic	Ritz Vectors	Normal Mode Shapes
Static Correction Term Included	First Vector is the Static Deflection	Large Number of Mode Shapes Needed
Spatial Contribution of Loading Included	Always	Depend on Direction of Applied Loads and Normal Modes
Computational Efficiency	More Efficient; Forward and Backward Substitution Required	Less Efficient; Eigen Solution Required
Size and Form of Reduced Equations of Motion	Small, Tri-Diagonal Mass Matrix, Diagonal Stiffness Matrix	Large, Diagonal Mass and Stiffness Matrices
Applied Load Restrictions	Limited To Locations of Static Loads	None

6.4 Techniques in Component Mode Synthesis

In this section, two model reduction techniques are briefly described because they are the most widely used in the payload component mode synthesis community.

Model Reduction

Model reduction can be performed by partitioning the mass, damping, and stiffness matrices into an “a”-set (analysis) and an “o”-set (omitted) as

$$M = \begin{bmatrix} M_{aa} & M_{ao} \\ M_{oa} & M_{oo} \end{bmatrix}, D = \begin{bmatrix} D_{aa} & D_{ao} \\ D_{oa} & D_{oo} \end{bmatrix}, \text{ and } K = \begin{bmatrix} K_{aa} & K_{ao} \\ K_{oa} & K_{oo} \end{bmatrix}. \quad (5.28)$$

Typically, the a-set partition corresponds to DOFs that are measured on the test structure.

The reduction transformation can be expressed as

$$\begin{Bmatrix} x_a \\ x_o \end{Bmatrix} = \begin{bmatrix} I \\ T_r \end{bmatrix} x_a. \quad (5.29)$$

Applying the above transformation to each of the property matrices, the results are

$$\begin{aligned} M_r &= M_{aa} + M_{ao}T_r + T_r^T(M_{oa} + M_{oo}T_r), \\ D_r &= D_{aa} + D_{ao}T_r + T_r^T(D_{oa} + D_{oo}T_r), \\ K_r &= K_{aa} + K_{ao}T_r + T_r^T(K_{oa} + K_{oo}T_r). \end{aligned} \quad (5.30)$$

Guyan Reduction Technique

Guyan reduction (Guyan 1965; Irons 1965) is one of the most widely used methods for model reduction. The popularity of this method is due in part to its simplicity. To determine the Guyan transformation T_G , it is assumed that all forces on the unmeasured (o-set) DOFs are equal to zero. The static problem can be written as

$$\begin{bmatrix} K_{aa} & K_{ao} \\ K_{oa} & K_{oo} \end{bmatrix} \begin{Bmatrix} x_a \\ x_o \end{Bmatrix} = \begin{Bmatrix} f_a \\ 0 \end{Bmatrix}. \quad (5.31)$$

Through matrix manipulation, the transformation that relates x_a to x_o can be determined as

$$x_o = -K_{oo}^{-1}K_{oa}x_a = T_G x_a. \quad (5.32)$$

Applying the Guyan transformation, the reduced stiffness and mass matrices can be written as

$$K_r = K_{aa} + K_{ao}T_G$$

and (5.33)

$$M_r = M_{aa} + M_{ao}T_G + T_G^T(M_{oa} + M_{oo}T_G).$$

Craig-Bampton Reduction Technique

The Craig-Bampton (Craig-Bampton 1968) reduction technique produced a hybrid reduced model with part physical part modal coordinates using the following transformation

$$T_{Cb} = \begin{bmatrix} I & 0 \\ T_G & \Phi_C \end{bmatrix}, \quad (5.34)$$

where Φ_C are modes computed with the interface points constrained.

REFERENCES

- Craig, R. R., Jr., and Bampton, M. C.,(1968), "Coupling of Substructures for Dynamic Analysis," AIAA Journal, Vol. 7, pp. 1313-1319.
- Guyan, R. J. (1965), "Reduction of Stiffness and Mass Matrices," AIAA Journal, Vol. 3, No. 2, pg. 380.
- Wilson, E. L., Yuan, M. W., and Dicken, J. M. (1982), "Dynamic Analysis by Direct Superposition of Ritz Vectors," Earthquake Engineering and Structural Dynamics, Vol. 10, pp. 813-821.